Conference Paper, Published Version

Islam, G. M. Tarekul; Kawahara, Yoshihisa; Uchida, Tatsuhiko; Morishita, Yu

2-D Simulation of Velocity Distribution in a Doubly Meandering Compound Channel Using CIP-Based Scheme

2-D SIMULATION OF VELOCITY DISTRIBUTION IN A DOUBLY MEANDERING COMPOUND CHANNEL USING CIP-BASED SCHEME

G.M. Tarekul Islam[1], Yoshihisa Kawahara[2], Tatsuhiko Uchida[3], and Yu Morishita[4]

[1] Visiting Researcher, Department of Civil and Environmental Engineering, Hiroshima University
1-4-1 Kagamiyama, Higashi Hiroshima, 739-8527, Japan, e-mail: x060053@hiroshima-u.ac.jp
[2] Professor, Department of Civil and Environmental Engineering, Hiroshima University
1-4-1 Kagamiyama, Higashi Hiroshima, 739-8527, Japan, e-mail: kawahr@hiroshima-u.ac.jp
[3] Associate Professor, Research and Development Initiative, Chuo University
1-13-27 Kasuga, Bunkyo-ku, Tokyo, Japan, email; utida@tamacc.chuo-u.ac.jp
[4] Engineer, River Engineering Division, Pacific Consultants Co., LTD
Azuchimachi, Chuo-ku, Osaka, 541-0052, Japan, e-mail: yuu.morishita@os.pacific.co.jp

ABSTRACT

Natural rivers often exhibit a meandering plan form. They are usually shaped to have a compound cross section for the purpose of flood control, navigation and environmental conservation. This results in a meandering compound channel. This paper explores the two-dimensional (2-D) numerical simulation of velocity distribution in a doubly meandering compound channel using the constrained interpolation profile (CIP) scheme. The experimental results of velocity distribution have been compared with the numerical results. It is found that the numerical scheme can simulate the 2-D velocity distribution in a doubly meandering compound channel reasonably well. Thus the present numerical method is likely to be applicable for predicting 2-D velocity distribution in a doubly meandering compound channel

Keywords: simulation, velocity, doubly meandering, compound channel, CIP-based scheme

1. INTRODUCTION

Natural rivers often exhibit a meandering plan form. They are usually shaped to have a compound cross section for the purpose of flood control, navigation and environmental conservation. This results in a meandering compound channel. When the main meander channel is flanked by floodplains with meandering levee, it results in a doubly meandering compound channel. Understanding of the hydraulics of meandering compound channels is important to design flood alleviation scheme.

Research has shown that the flow structure is complex, even for straight compound channels. It has been pointed out that at a low floodplain depth the large velocity difference between the main channel and the floodplain induced a strong shear layer and a lateral momentum transfer across the interface between the main channel and the floodplain (Knight and Demetriou, 1983; Wormleaton and Merrett, 1990). The flow mechanisms are more complex for meandering compound channel due to an increase in the three-dimensional nature of the flow, the interaction between the flow in the main channel and the floodplain and the unsteady nature of flow. Many researches have been conducted to understand the complicated flow structures in compound meandering channel with straight floodplain (Kiely, 1990; Willets and Hardwick, 1990; Sellin et al. 1993; Ishigaki et al., 1997). But little is known about the flow structures in a doubly meandering compound channel. The flow structures become even more complex when there is a difference in phase between alignments of main channel and that of outer levees. Kinoshita (1988) made experiments focusing on the

phase difference between the main channel alignment and the levee alignment. He investigated the effects of the phase shift on the meandering channel flows from standpoint of surface velocity and bed evolution. Fukuoka and Ohgushi (1997) studied the effect of levee alignment on meandering compound channel flows. They studied two cases of flow which had different phase of meandering between levees and main channel. Dead water area was found in the first case, where the meandering of levee goes ahead of that of main channel. In the second case, where the meandering of levees goes behind, the flow is found to occur over the channel. Manson and Pender (1997) presented a computational study of turbulent free surface flow in a meandering compound channel. Their simulation could not capture the motions in the cross-over region. Shao et al. (2003) performed numerical modeling of turbulent flow in curved channels of compound cross-section. Sugiyama et al. (2006) carried out numerical analysis of turbulent structure in compound meandering open channel by an algebraic Reynolds stress model.

The flow in a meandering compound channel is characterized by accelerating and decelerating flows. The CIP (the constrained interpolation profile or the cubic interpolated pseudo-particle /propagation) scheme (Yabe et al., 1990) is capable of computing the advection term with high accuracy. The CIP scheme has attracted a great deal of attention. This paper deals with simulation of 2-D velocity distribution in a doubly meandering compound channel using CIP-based scheme (Uchida and Kawahara, 2006; Uchida, 2006). The scheme enables one to capture the effects of the distributed parameters, such as velocities, water depth and boundaries, in the governing equations even by Cartesian grid system. The accuracy of the scheme is assessed by comparing the results with the measured data on velocity distribution in a large experimental flume of a doubly meandering compound channel.

2. EXPERIMENTAL SETUP

The experiments were conducted in a tilting flume whose length, width and depth are 30 m, 1.5 m and 1 m, respectively. Figure 1 shows the general layout of the experimental channel. The flume constructed with vinyl chloride was mounted on 2 m steel channel structures. The longitudinal gradient of the channel is adjustable with a jack and hinge and can be varied up to 5%. The channel consists of a main channel flanked by meandering levee on both sides of the main channel. The outer levee which has the same sinuosity as of main meander channel has a phase difference of about 30^0 ahead of main channel. The meanders are expressed as combinations of arcs and straight reaches. The flume consists of nine consecutive meandering waves with straight approach channels at the beginning and end of the meandering part of the channel. The bed of the main channel and floodplains is smooth. The width and depth of the main channel are 30 cm and 5 cm, respectively. The angle of arc is 60^0 with a sinuosity of 1.05. The longitudinal gradient of the flume was set to 1/1000. Figure 2 shows the definition sketch of different geometric parameters. The magnitudes of different geometric parameters are shown in Table 1. The details can be found in Islam (2000).
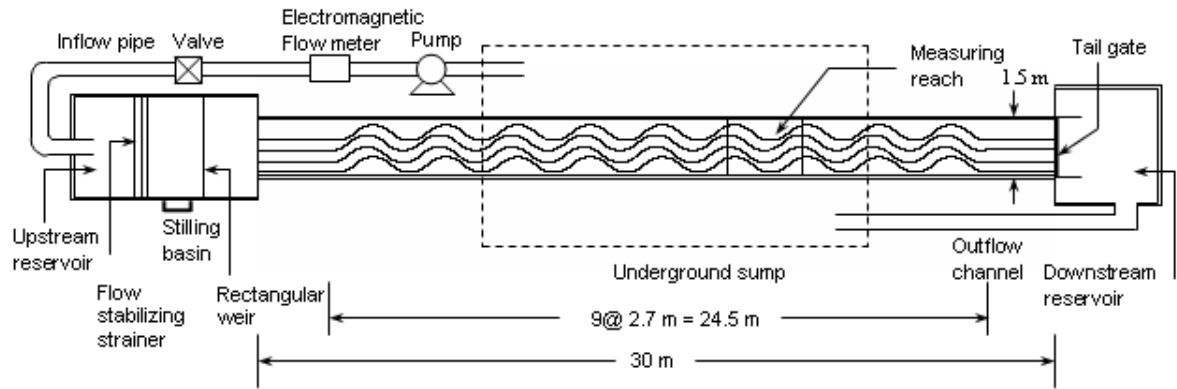
Figure 1 General layout of the experimental setup.
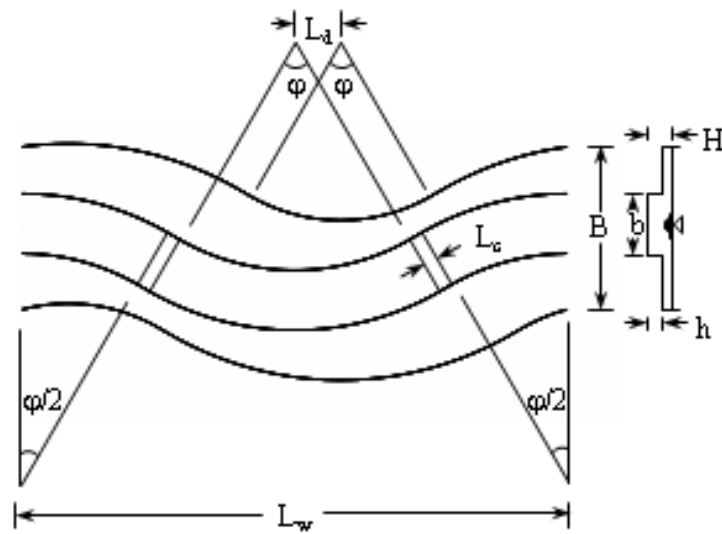
Figure 2 Geometric parameter in one meander wave.

Table 1 Geometric parameters of the compound meandering channel.

Parameters	Dimension
Meander wavelength	$L_w = 2.720$ m
Curved channel length	$L = 2.863$ m
Cross-over length	$L_c = 0.070$ m
Phase difference	$L_d = 0.229$ m
Total width	$B = 0.800$ m
Channel width	$b = 0.300$ m
Height of floodplain	$h = 0.050$ m
Sinuosity	$S = 1.05$
Angle of arc	$\varphi = 60^0$
Main channel inner radius	$R_{mi} = 1.150$ m
Main channel outer radius	$R_{mo} = 1.450$ m
Flood levee inner radius	$R_{fi} = 0.900$ m
Flood levee outer radius	$R_{fo} = 1.700$ m

For the measurement of water levels and velocities, the measuring probes were mounted on a carriage which travelled along the flume on a rail system. The movement of the carriage in the transverse and vertical direction is automatically performed by electric motor which can be programmed to move the probe to the desired position. The accuracy of positioning of the measuring probe to the desired location is 0.01 cm. A point gauge was used to measure the channel bed elevations while a position meter was used to measure water surface elevations. The mean depth was assumed to be the difference between the mean bottom and mean water surface elevations. The accuracy of the position meter was 0.01 cm. An electromagnetic flow meter installed in the outflow pipe was used to measure the instantaneous discharge.

The velocities were measured by two-component electromagnetic current meter. The I-type probe was used for measuring x- and y-velocity components. The x-velocity is in the direction normal to each cross section while the y-velocity is in the direction parallel to the cross section. The measuring time for velocity measurement was 40 seconds with a sampling frequency of 5 Hz. The data were then averaged to get the point velocities.

As the main channel meander is regular, the flow field is considered to be the same at positions in phase after the flow is fully developed. Thus the measuring reach has been selected at a distance of about 15 m from the beginning of the meander channel to ensure fully developed flow condition. The measurements were conducted over a measuring section of one wavelength i.e., 2.72 m. The measuring reach has been divided into 9 sections. The part of the section on the floodplain is normal to the longitudinal direction of the channel. Sections 1, 5 and 9 are called as the bend apex sections while sections 3 is the first cross-over section while section 7 is the second cross-over section.

Two flow conditions were considered viz.: shallow water condition and deepwater condition. In shallow water condition the average depth of flow over the floodplain is 0.94 cm whereas in deepwater condition it is 4.85 cm. The average depth of flow over the floodplain 4.85 cm for deepwater condition was selected by assuming that during flood the average depth of flow over the floodplain could be as high as the depth of bank-full flow. The flow conditions are summarized in Table 2.

Table 2 Flow conditions.

Flow conditions	Shallow	Deep
Average depth, cm	5.94	9.85
Discharge, m^3/s ($\times 10^{-3}$)	7.50	26.33
Relative depth, Dr	0.16	0.49
Mean velocity, m/s	0.326	0.479
Reynolds number, Re ($\times 10^4$)	0.813	2.600
Froude number, Fr	0.658	0.652

3.   NUMERICAL MODEL

The governing equations of two-dimensional unsteady flows with complex impermeable boundaries are described by the following shallow water equations, which are identical to those in the FAVOR Method (Hirt, 1992):

$$\frac{\partial fh}{\partial t} + \frac{\partial u_j \cdot fh}{\partial x_j} = 0 \tag{1}$$

$$\frac{1}{fh}\left(\frac{\partial fu_i h}{\partial t}+\frac{\partial u_j \cdot fu_i h}{\partial x_j}\right)=-g\frac{\partial \zeta}{\partial x_i}-\frac{\tau_{0i}}{h}+\frac{\partial \tau_{ij}h}{h\partial x_j} \tag{2}$$

where subscripts i,j follow the summation convention, indicating $1=x$ and $2=y$, respectively; $h=$ water depth; $u_i=$ velocity along x_i direction; $f=$ occupancy ratio of fluid; $g=$ acceleration due to gravity; $\zeta=$ water surface elevation $(h+z)$; $z=$ ground elevation; $\tau_{0i}=$bed shear stress ; and $\tau_{ij}=$ horizontal shear stress tensor due to molecular and turbulent motion of fluids.

In this study, bed shear stress is expressed by the Manning equation. The Reynolds stresses are represented by the kinematic eddy-viscosity coefficient.

$$\tau_{ij}=2\nu_t S_{ij}-2/3\delta_{ij}k \tag{3}$$

$$S_{ij}=\frac{1}{2}\left(\frac{\partial u_i}{\partial x_j}+\frac{\partial u_j}{\partial x_i}\right) \tag{4}$$

$$\nu_t=\nu+\left(C_s^{\ 3}C_\varepsilon\right)^{1/3}\Delta k^{1/2} \tag{5}$$

$$\frac{\partial k}{\partial t}+u_j\frac{\partial k}{\partial x_j}=\frac{1}{hf}\frac{\partial}{\partial x_i}\left(\nu_t hf\frac{\partial}{\partial x_i}\right)+\nu_t\left(2S_{ij}^{\ 2}\right)+\frac{C_0 u_*^{\ 2}\sqrt{u_i^{\ 2}}}{h}-C_\varepsilon\frac{k^{3/2}}{\Delta} \tag{6}$$

where ν, $\nu_t=$ kinematic viscosity coefficient and kinematic eddy-viscosity coefficient, respectively; $k=$ depth averaged turbulent energy; $\kappa=0.4$, Karman's constant; C_s, Smagorinsky's constant $(C_s=0.5)$; $C_\varepsilon=1.0$; $\Delta=(dxdy)^{1/2}$; $u_*=(\tau_{0i}^{\ 2})^{1/2}$, friction velocity. C_0 is defined to adapt the term to 0-equation model $(\nu_t=\alpha u_* h,\ \alpha=\kappa/6)$ as Eq. (7).

$$C_0=\alpha^3\left(\frac{h}{\Delta C_s}\right)^4\frac{u_*}{\sqrt{u_i^{\ 2}}} \tag{7}$$

Figure 3 shows a computational grid consisting of permeable and impermeable areas together with the arrangement of main variables in the grid. All the variables in the governing equations are set on the same location. Each control volume ij has three kinds of variables, i.e., the value at the intersection of the grid (Point Value (P), denoted by lower-case characters), the averaged value along the side of the grid (Line-averaged Value (L_xa, L_ya), denoted by capital letters with subscript of x or y) and the averaged value over the grid (Area-averaged Value (Aa), denoted by capital letters with subscript of xy). The interpolating operation of the variables, which has frequently been utilized in many numerical schemes based on the staggered grid, including the original CIP scheme, is not necessary in the present scheme. Any boundary conditions can be taken into account with those distributions in the cell by using multi-valuables. In the original CIP scheme for the shallow water equations, the advection terms are transformed from conservative form into non-conservative form to eliminate water depth h in the advection terms, with the help of the Continuity Equation (1). In the present scheme, time variation of the depth-integrated momentums and water depths are computed directly by CIP-CSL2 (Nakamura et al., 2001) without the transformation of the advection terms. The computation was carried out with a numerical mesh covering the entire flow channel. The grid size was 8 cm × 5 cm. The boundary conditions were provided in terms of the upstream and downstream water levels.

Figure 3 labels:

δx

Impermeable wall

δy

$F_{xij} \cdot \delta y$

$F_{xi+1j} \cdot \delta y$

U_{yi+1j}

$F_{xyij} \cdot \delta x \delta y$

U_{yij}

V_{xij}

$F_{yij} \cdot \delta x$

$L_y a : H_{yij}, U_{yij}, V_{yij}, F_{xij}$

$ij+1$

δx_{ij}

$Aa : V_{ij}, H_{xyij}$

δy_{ij}

U_{xyij}, F_{xyij}

$i-1j$

ij

$i+1j$

$P : u_{ij}, \upsilon_{ij}, h_{ij}, f_{ij}$
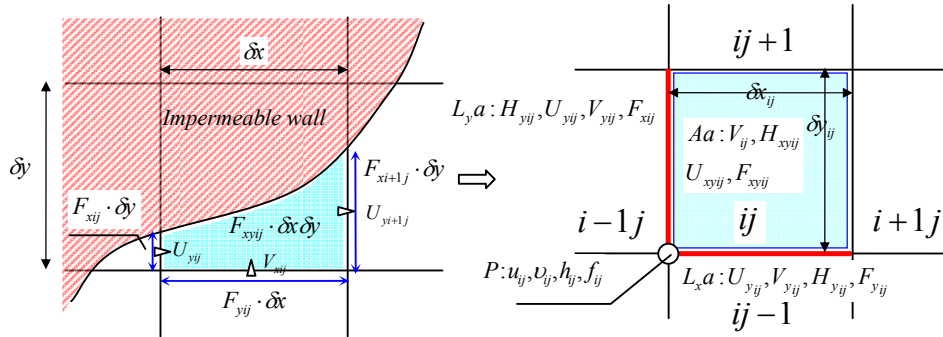
$L_x a : U_{yij}, V_{yij}, H_{yij}, F_{yij}$

$ij-1$

Figure 3 Computational grids with impermeable walls and the arrangement of main variables on the volume ij.
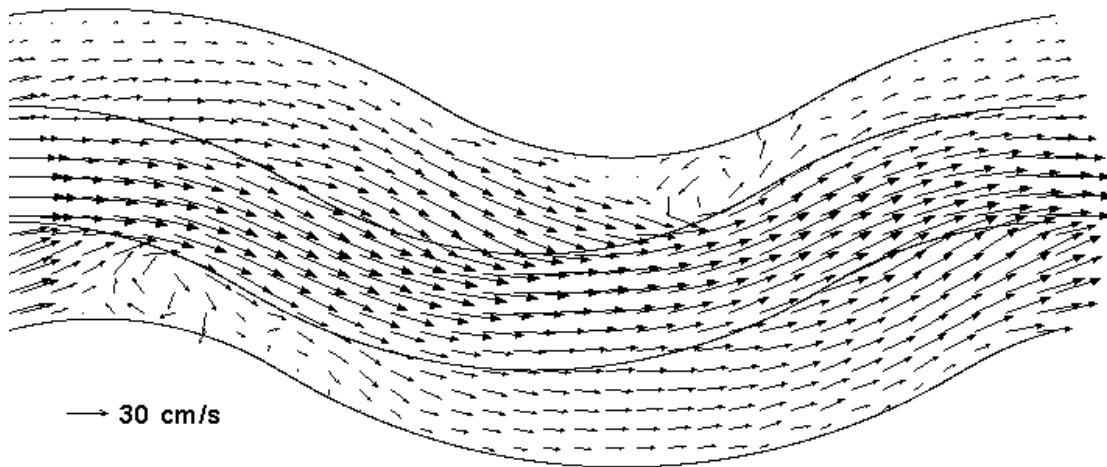
4.   RESULTS AND DISCUSSIONS

Figures 4(a) and (b) show the distribution of depth-averaged 2-D velocity fields under shallow water condition for experiments and simulation, respectively. The 2-D velocity is the resultant of the x-velocity (u) and the y-velocity (v) components. The velocity fields show that the maximum velocity occurs near the inner bank of the main channel while the minimum velocity occurs near the outer bank for both experiments and simulation. If the positions of the maximum velocity filaments at different sections are joined together, it appears to follow the shortest route. The difference of magnitudes of the maximum and minimum velocities in the main channel is minimum at section 2 while it is maximum at section 4. The flow fields in the cross-over section follow the alignment of the main channel. This means that the flow fields are perpendicular to the section at the point of inflection where the curvature effect is non-existent. The flow patterns are virtually the same at the next half of the meander wave but in opposite orientation. By comparing the experimental and simulated results, it is seen that the simulation can reproduce the transverse and longitudinal 2-D velocity distribution reasonably well.

In the bend apex section, the simulated primary velocity (u) slightly under predicts in the left hand side from the centreline of the main channel while it over predicts in the right hand side from the centreline of the main channel. The model simulates primary velocity (u) better than lateral velocity (v). In addition, as the boundary conditions were provided by the upstream and downstream water levels, the calculated discharge (0.0067 m³/s) differs with the measured discharge (0.0075 m³/s). These can be attributed to the fact the present model is 2-D while the flow in a doubly meandering compound channel is 3-D. Anyway, the simulated results are in close agreement with the experimental results. Therefore, the present numerical method is likely to be applicable for predicting 2-D velocity fields in a doubly meandering compound channel.

Due to the limitation of the instrument, it was not possible to measure the velocity fields over floodplain under shallow water condition. And thus it was not possible to know the strength and position of horizontal circulation over the floodplain. From the simulated results, it is seen that 2-D velocity distribution under shallow water condition is characterised the two well developed circulations or eddies. The width of the eddy at its center covers the whole floodplain width while the length of the eddy covers around one-forth of the meander wave. The formation of the eddy is confined in the floodplain only.
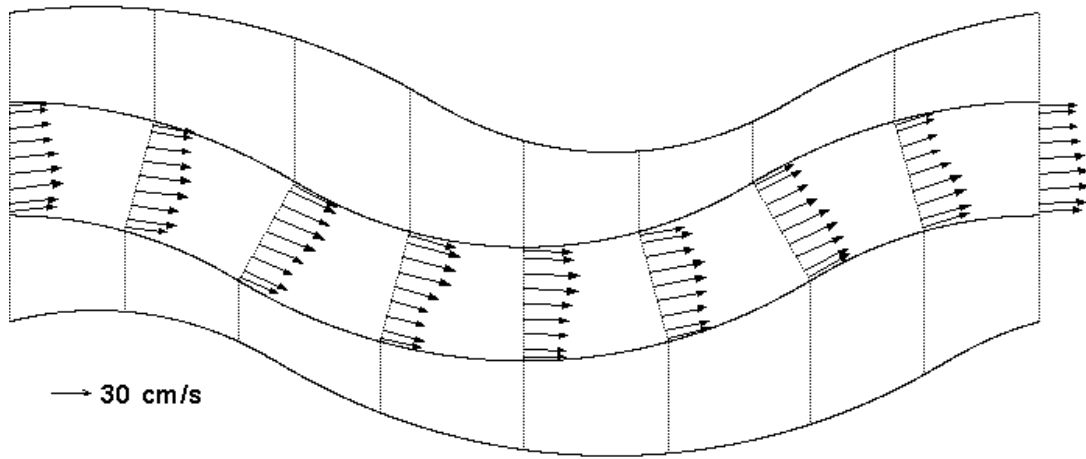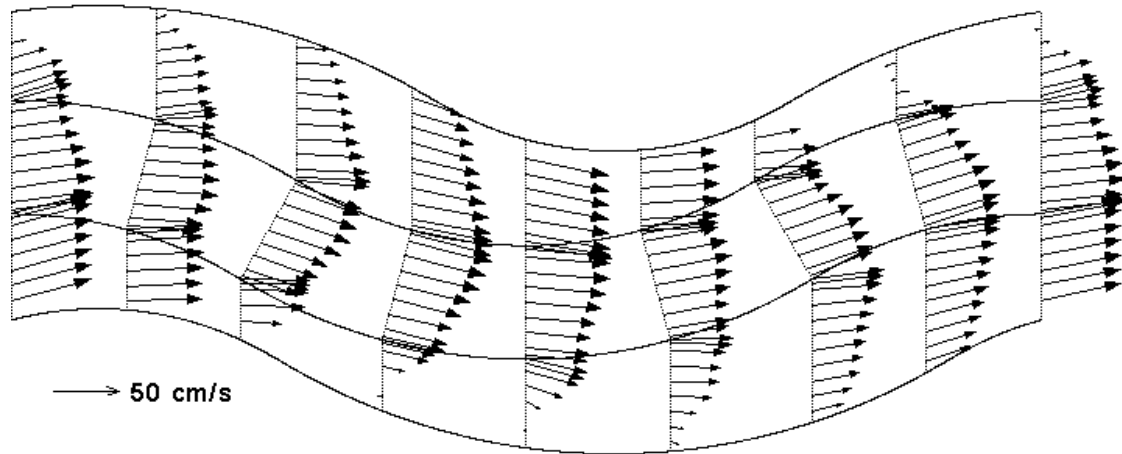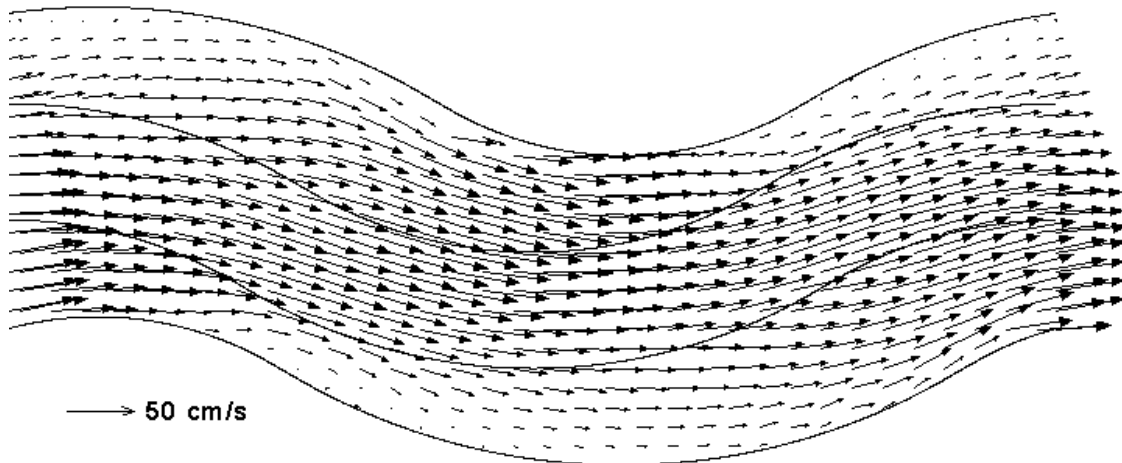
(a) Experiment

(b) Simulation

Figure 4 Comparison of experimental and simulated velocity distribution under shallow water condition (Dr = 0.16).

Figures 5(a) and (b) show the depth-averaged stream-wise velocity distribution of 2-D velocity fields for deep water condition for experiment and simulation, respectively. The flow fields at the bend apex sections show that the maximum velocity occurs near the inner bank of the main channel while the minimum velocity occurs near the outer bank. The results show that the simulation can capture this phenomenon quite well. The difference of magnitudes of the maximum and minimum velocities in the main channel is maximum at the bend apex section while it is minimum at the cross-over section. This suggests that the flow pattern in a doubly meandering compound channel depends on the amount of flow over the floodplain. The flow fields in the cross-over section follow the alignment of the main channel. This means that the flow fields are perpendicular to the section at the point of inflection where the curvature effect is non-existent. The flow patterns are virtually the same at the next half of the meander wave but in opposite orientation. By comparing the experimental and simulated results, it is seen that the simulation can reproduce the transverse and longitudinal 2-D velocity distribution reasonably well.

(a) Experiment

(b) Simulation

Figure 5 Comparison of experimental and simulated velocity distribution under deep water condition (Dr = 0.49).

In the bend apex section, the width of the right floodplain gradually narrows down and the velocity filament tends to retard to the main channel from floodplain which causes vigorous mixing of floodplain flow to the main channel flow. The mixing is high at the interface between main channel and floodplain at the right bank at the cross-over region where the width of the floodplain gets far narrower. The width of the right floodplain at the cross-over section gradually increases in the downstream direction until the next cross-over section is reached. Consequently, the degree of deviation of the velocity filament becomes weaker and follows the main channel alignment. On the other hand, the width of the left floodplain at the bend apex gradually increases in the downstream direction until the cross-over section is reached. This causes the main channel flow to enter into the floodplain. The opposite things happen in the next bend. The comparison of the experimental and simulated results shows that the simulation can reproduce the transverse and longitudinal 2-D velocity distribution under deep water condition reasonably well.

The results show that the simulated primary velocity (u) over predicts in the bend apex section, but it can capture the velocity pattern quite well. Also the results show that the model simulates primary velocity (u) better than lateral velocity (v). Besides, the calculated discharge (0.0224 m^3/s) differs with the measured discharge (0.0263 m^3/s). This can be attributed to the fact the present model is 2-D while the flow in a doubly meandering compound channel is 3-D. However, the present numerical method is likely to be applicable for predicting 2-D velocity distribution in a doubly meandering compound channel.

It is seen that the distribution of stream-wise velocities under deep water condition is characterized by the formation of two well-defined circulations or eddies as in the shallow water condition. The width of the right floodplain immediately after the cross-over region widens in the downstream direction. The flow in this region behaves like a flow separation and thus causes the velocity filaments to reverse the direction near the levee wall. The width of the eddy at its center appears to be half of the floodplain width. The position and strength of these eddies also depend on the water depth above floodplain. When the depth of water over the floodplain increases, the strength of this horizontal eddies diminish as the main flow dominates everywhere in the channel. With higher water depth, the horizontal eddies appear to suppress and confine to a position upstream of the bend apex. The simulation can reproduce this phenomenon reasonably well.

5.   CONCLUSIONS

This paper explores the two-dimensional (2-D) numerical simulation of velocity distribution in a doubly meandering compound channel. The velocity fields under shallow water condition show that the maximum velocity occurs near the inner bank of the main channel while the minimum velocity occurs near the outer bank for both experiments and simulation. The difference of magnitudes of the maximum and minimum velocities in the main channel under shallow water condition is minimum at section 2 while it is maximum at section 4. By comparing the experimental and simulated results, it is seen that the simulation can reproduce the transverse and longitudinal 2-D velocity distribution reasonably well.

The flow fields at the bend apex sections under deep water condition show that the maximum velocity occurs near the inner bank of the main channel while the minimum velocity occurs near the outer bank. The difference of magnitudes of the maximum and minimum velocities in the main channel is maximum at the bend apex section while it is minimum at the cross-over section. The results show that the simulation can capture this phenomenon quite well. The present numerical method is likely to be applicable for predicting 2-D velocity fields in a doubly meandering compound channel.

From the simulated results, it is seen that 2-D velocity distribution under shallow water condition is characterised the two well developed circulations or eddies. The width of the eddy at its center covers the whole floodplain width while the length of the eddy covers around one-forth of the meander wave. The formation of the eddy is confined in the floodplain only. The 2-D velocity distribution under deep water condition is characterized by the formation of two well-defined circulations or eddies as in the shallow water condition. The position and strength of these eddies also depend on the water depth above floodplain. When the depth of water over the floodplain increases, the strength of this horizontal eddies diminish as the main flow dominates everywhere in the channel. With higher water depth, the horizontal eddies appear to suppress and confine to a position upstream of the bend apex. The simulation can reproduce this phenomenon reasonably well.

REFERENCES

Fukuoka, S. and Ohgushi, H. (1997), Effect of levee alignment on doubly meandering compound channel flows, *Annual Journal of Hydraulic Engineering*, JSCE, 41, pp.1137-1140.

Hirt, C. W. (1992), Volume-fraction techniques: powerful tools for wind engineering, *Journal of Wind Engineering*, 52, pp.333-344.

Ishigaki, T., Muto, Y., Takeo, N. and Imamoto, H. (1997), Fluid mixing and boundary shear stress in compound meandering channel, in *27th Congress of IAHR*, San Francisco, USA, pp.763-768.

Islam, G.M.T. (2000), Three-dimensional Flow Fields in a Doubly Meandering Compound Channel under Steady and Unsteady Flow Conditions, *Ph.D. dissertation*, Department of Civil Engineering, University of Tokyo, Japan.

Kiely, G. (1990), Overbank flow in meandering compound channels: the important mechanisms, Ed. White, W.R., Wiley, Chichester, pp.207-213.

Kinoshita, R. (1988), Experimental study concerning field work of alluvial phenomena at flooding and best possible river course example. *Report of Scientific Research*, pp.63-168.

Knight, D.W. and Demetriou, L.D. (1983), Flood-plain and Main Channel Flow Interaction, *J. Hydraulic Engineering*, ASCE, 109(8), pp.1073-1092.

Nakamura, T., Tanaka, R., Yabe, T. and Takizawa, K. (2001), Exactly conservative semi-Lagrangian scheme for multi-dimensional hyperbolic equations with directional splitting technique, *Journal of Computational Physics*, 174, pp.171–207.

Nezu, I. and Nakagawa, H. (1993), *Turbulence in open channel flows*, IAHR Monograph, Belkema, Rotterdam, Netherlands.

Manson, J.R. and Pender, G. (1997), Three dimensional modeling of flow and transport mechanisms in meandering two-stage channel flow, in *27th Congress of IAHR*, USA, pp. 835-840.

Shao, X., Wang, H. and Chen, Z. (2003), Numerical modeling of turbulent flow in curved channels of compound cross-section, *Advances in Water Resources*, 26, pp.525-539.

Sellin, R.H.J., Ervine, D.A., and Willetts, B.B. (1993), Behaviour of meandering two-stage channels, Proc. Instn Civ. Engrs, *Water, Maritime. & Energy*, 101, pp.99-111.

Sugiyama, H., Hitomi, D. and Saito, T. (2006), Numerical analysis of turbulent structure in compound meandering open channel by algebraic Renolds stress model, *International Journal for Numerical Methods in Fluids*, 51, pp.791-818.

Uchida, T. and Kawahara, Y. (2006), Development of an explicit conservative CIP scheme for shallow water flows, *Journal of Applied Mechanics*, JSCE, 9, pp.917-924, in Japanese.

Uchida, T. 2006. A CIP－based method for shallow water flows in complex Geometries using Cartesian grids, in *Proceedings of the 7th International Conference on HydroScience and Engineering*, *Philadelphia*, ICHE 2006.

Wormleaton, P.R. and Merrett, D. (1990), An Improved Method of Calculation of Steady Uniform Flow in Prismatic Main/Flood Channel Plain Sections, *Journal Hydraulic Research*, 28, pp.157-174.

Willets, B.B. and Hardwick, R.I. (1990), Models studies of overbank flow in meandering channels, Proc. Institution of Civil Engineers, *Water, Maritime and Energy*, 101, pp.45-54.

Xiao, F., Yabe, T. and Ito, T. (1996), Constructing oscillation preventing scheme for advection equation by rational function, *Computer Physics Communications*, 93, pp.1-12.

Yabe, T., Ishikawa, T. and Kadota, Y. (1990), A multidimensional cubic-interpolated pseudoparticle (CIP) method without time splitting technique for hyperbolic equations, *Journal of the Physical Society of Japan*, 59(7), pp.2301-2304.